Journal of Applied Electrochemistry **31**: 559–564, 2001.

Effect of particles on polarization during electrocodeposition using a rotating cylinder electrode

JEAN L. STOJAK** and JAN B. TALBOT*
Chemical Engineering Program, University of California, San Diego, 9500 Gilman Drive, La Jolla, CA 92093-0411, USA
*(*author for correspondence)*
*(**at Composite Optics, Inc., San Diego, CA 92121, USA)*

Received 12 June 2000; accepted in revised form 21 November 2000

Key words: alumina particles, electrodeposition, mass transfer, polarization, rotating cylinder electrode

Abstract

The influence of suspended submicrometric diameter alumina particles on polarization during electrocodeposition with copper at a rotating cylinder electrode was investigated. Cathodic polarization and mass transfer experiments were conducted as a function of electrode rotational speed and particle loading.

1. Introduction

Most studies of electrocodeposition have focused on maximizing particle incorporation in the electroplated metal matrix or improving a specific property of the composite film, such as better corrosion or oxidation resistance, lower wear rates, and overall increase in the longevity of the coating. For electrolytes without bath additives, particle incorporation levels typically range from 1–10 vol %. This level of incorporation requires a concentration of particles suspended in the plating bath ranging from 2–200 g l^{-1} depending on the desired composition of the film [1–11]. There are few reports that directly compare polarization curves with and without particles, except to state that during deposition of insulating particles the surface area for electrodeposition decreases, and thus, current decreases; whereas during incorporation of conducting particles the surface area increases and hence, so does current [12]. The effect of chromium particles (~1–2 μm average diameter) on nickel electrodeposition on a rotating cylinder electrode has been studied [9]. The addition of chromium particles to the bath was found to shift the cathodic polarization curves to more positive potentials, ~50 mV for 0.1 vol % and ~100 mV for 4.2 vol % particles in solution for all of the nickel bath concentrations studied. It was concluded that chromium particles catalysed nickel electrodeposition [9]. In a study of electrocodeposition of ~3 μm diameter SiC particles in cobalt it was observed that there was no significant effect of particle content (up to 5 g l^{-1}) on the polarization curves, in which up to 5 wt % of particles was occluded [13].

Both mass transfer and the effect of particles on mass transfer have been studied by measuring limiting current density for a variety of fluid flow geometries, however, not also with incorporation of the particles in an electrodepositing metal. The mass transfer studies with a rotating cylinder electrode (RCE) are of particular interest as they pertain to the experimental system used in our study. Mass transfer (without particles) between concentric cylinders of which the inner cylinder is rotated was first studied by Eisenberg, Tobias, and Wilke (ETW) in 1954 [14]. Their work provides an empirical correlation for $835 < Sc < 11{,}500$ and $112 < \mathrm{Re} < 241{,}000$ (with an average error of $\pm 8.3\%$) for limiting current density (i_L):

$$i_L = 0.0791 \frac{nFDC}{2r_i} Sc^{0.356} Re^{0.7} \quad (1)$$

where n is the number of electrons involved in the electrochemical reaction, F is the faradaic constant, D is the reactant diffusion coefficient, C is the bulk reactant concentration, and r_i is the radius of the inner electrode, respectively. The Schmidt number, Sc, and the Reynolds number, Re, are defined as $Sc = \nu D^{-1}$ and $Re = 2\omega r_i^2 \nu^{-1}$, where ν is the kinematic viscosity of the fluid and ω is the rotational speed of the inner cylinder.

There are three possible ways to define the characteristic length in Re for a concentric cylinder cell: (i) the rotating electrode radius, (ii) the electrode height, or (iii) the gap distance between electrodes. Eisenberg, Tobias and Wilke [14] showed that the best correlation of the data is obtained when the characteristic length is the radius of the rotating cylinder. However, Newman [15] argued that the ratio of the inner to the outer cylinder diameters should be incorporated into the ETW correlation, as follows:

$$i_L = 0.0791 \frac{nFDC}{2r_i} \left(\frac{r_i}{r_o}\right)^{0.7} Sc^{0.356} Re^{0.7} \quad (2)$$

Nevertheless, Gabe and Robinson [16] believed that the correction to the *Re* number is unnecessary since any effect of the radius ratio would be incorporated as a change in the value of the constant of the empirical relationship in Equation 1. Furthermore, the ETW correlation obtained the 0.0791 value for the constant using a range of inner to the outer radius ratios from 0.09 to 0.8.

The ETW correlation has been confirmed by several investigators, however slight variations in the values of the power indices have been reported [17–19]. The power of the *Sc* number ranges from 0.3 to 0.4, and the power of the *Re* number ranges from 0.59 to 0.7. The surface roughness is thought to have an effect on the correlation, since it affects the friction factor. This may be a consideration during electrocodeposition, as particles may affect the surface roughness of the deposit.

The mass transfer enhancement due to the addition of inert particles at a RCE has been investigated [20]. The effects of rotational speed, and particle size, density and loading were determined by limiting current density measurements for ferricyanide reduction. Transport enhancements of up to 2.5 times were observed with 5–80 μm diameter microspheres, which were attributed to the microconvective eddies produced by particle rotation in the shear field adjacent to the RCE, and to the increased shear rate caused by the formation of a particle-free wall layer. The particle radius, a, was chosen as the proper characteristic length. Therefore, experimental data were generally correlated for concentrated suspensions containing 10–40 vol % solid particles by

$$i_L = \frac{\alpha(\phi) nFDC}{a} Sc^{0.33} Re_a^{\beta(\phi)} \quad (3)$$

where α and β are functions of particle loading volume fraction, ϕ. However, for a particle loading less than 30%, a simpler relationship may be used (with an average error of $\pm 13\%$):

$$i_L = \frac{\alpha nFDC}{a} Sc^{0.33} Re_a^{0.43} \quad (4)$$

where α is 0.03, 0.046 and 0.069 for particle loadings of 10, 20 and 30 vol %, respectively. The kinematic viscosity in the Schmidt number is based on the suspension properties and the Reynolds number is defined as $Re_a = a^2 r_i^{1.4} \omega^{1.7} \nu^{-1.7}$. As noted in the article [20], a particle-free wall layer would not form in the case of a suspension with particle diameters less than 1 μm. The effects of small, colloidal particles on mass transport rates has not yet been studied.

To optimize the bath composition for a study of the parameters that affect the electrocodeposition of alumina particles within a copper matrix using a RCE system, cathodic polarization and mass transfer experiments were conducted as a function of electrode rotational rate, bath chemistry, and particle loading [21, 22]. A concentric RCE cell used in this work was operated under conditions of turbulent flow. In general, the advantages of a RCE system (over the more popular RDE) are that both the primary and mass-transfer limited current distributions are uniform, and both the ohmic potential drop and the concentration change at the electrodes can be calculated even though the flow is turbulent [15]. Copper was chosen as the matrix metal as acid copper plating baths have high current efficiency ($\sim$100%) and for certain bath chemistries mass transfer limited rates can be reached before the onset of hydrogen evolution. Of course, the particles (50 nm diameter alumina) in our study are also being incorporated (up to 4.4 wt %) into the electrodeposit. Our results will be discussed in light of previous mass transfer studies conducted with a RCE with and without the effects of particles.

2. Experimental details

Experiments were conducted using a three electrode system, consisting of a RCE, a concentric stationary electrode, and a saturated calomel reference electrode (SCE) placed in a Luggin capillary, which was positioned flush with the cell wall to minimize disturbance to the flow [22]. The inner rotating electrode was a removable stainless steel cylinder, machined to a diameter of 12 mm and 8 mm in height with a Teflon encapsulated shaft. The surface of the rotating cylinder electrode was recessed slightly (20 μm) from the Teflon surfaces above and below it, in order to reduce the effect of the current discontinuity at the electrode edges. The primary current distribution was calculated for the experimental concentric cylinder configuration [21, 22]. Oxygen-free high-conductivity copper foil was used to make the stationary outer cylindrical anode. The stationary anode, positioned flush against the inside of the cell wall to minimize flow disturbance, was 9 mm high with an inner radius of 24 mm. Insulating tape was used to cover the outside surface of the cylindrical anode foil, as well the submerged portion of the electrical connection and support for the anode. Our system has a radius ratio of 0.2 which within the range evaluated by ETW [14].

An EG&G PAR potentiostat/galvanostat (model 273) was used to control the voltage and to monitor the corresponding current. The current and voltage measurements were recorded using a computer data acquisition system.

All glassware was first cleaned in a solution of sulfuric acid, nitric acid, and distilled deionized (DDI) water with a 4:2:1 volume ratio. This was followed by five thorough rinses with deionized water before a final rinse with DDI water. The stainless steel cathodes were polished to a 1 μm finish using a slurry of alpha-alumina

in DDI water and then buffed using Wenol® polish. The cathodes were degreased by soaking in methanol for 30 min, rinsed with DDI water, and then soaked in isopropanol for 30 min. Just prior to the polarization experiment, the cathode was soaked in 0.1 M sulfuric acid for 5 min, rinsed in DDI water, and dried using an inert gas (nitrogen or argon). The anodes were degreased in the same manner as the cathodes. Just prior to the polarization experiment, the anodes were soaked in 0.1 M sulfuric acid for 5 min, rinsed with DDI water, dried with a lint free tissue, and positioned into the cell which was then immediately filled with the electrolyte to be analysed.

Mass transfer studies have been conducted using copper sulfate baths [20, 23–26]. However, the concentration of the copper sulfate was typically very low (l–l0 mM), generally with an excess of sulfuric acid present. Without acid present in the bath the onset of hydrogen evolution occurs before the mass transfer limited copper deposition is reached. The low copper concentrations used in these earlier studies restricted the investigations to low reaction rates [23–25]. Since industrial application of electrocodeposition would be impractical at these low rates, higher copper concentrations were desired for this work. Polarization scans were conducted using the RCE system to optimize the bath composition, allowing the full range of deposition to be studied without the complications due to the onset of hydrogen evolution [21]. The optimized bath composition was determined to be 0.1 M $CuSO_4$ + 1.2 M H_2SO_4.

Fresh electrolyte was prepared for each experiment using reagent grade sulfuric acid and copper sulfate. The pH was adjusted to a value of 0.30 ± 0.01 using sulfuric acid. Suspensions were prepared by adding 200 ml of solution into a 250 ml beaker and adding a specified weight of particles. The mixture was covered and stirred using a magnetic stirrer for 12–24 h, placed in an ultrasonic bath for 15 min, and cooled to room temperature. Temperature and pH of the suspensions were recorded before and after each experiment. Conductivity was measured for the suspensions using a Yellow Springs Instrument (YSI) conductivity probe (model 3401), in conjunction with a YSI conductivity meter (model 34).

Limiting current density was measured for particle loadings of 3.9, 19.5, 39, 120 and 158 g l^{-1} (corresponding to 0.12, 0.59, 1.2, 3.5 and 4.6 vol % in solution) at three electrode rotational rates: 500, 1000 and 1500 rpm. Settling of particles occurred with loadings greater than 158 g l^{-1}. For a 6 mm radius rotating cylinder, the onset of turbulence occurs at a rotational rate of 60 rpm. The smallest sized gamma phase alumina powder available, 50 nm diameter supplied by Buehler, Ltd, was used. It was determined that this powder was actually a mix of α and γ phases with a density of 3.3 g cm^{-2} [21, 22].

Polarizations were measured without particles and with particle loadings of 39, 120 and 158 g l^{-1} and electrode rotational rates of 1000 and 1500 rpm. Just prior to the polarization scans, a preliminary scan was conducted from the open circuit potential to −0.3 mV vs SCE at 5 mV s^{-1}, then held at −0.3 mV for 90 s in a 0.1 M acid copper sulfate bath (pH 0.3), without particles. This preliminary scan was conducted to obtain a fresh copper surface thick enough (0.73 μm) to eliminate the capacitive response obtained when using a stainless steel cathode [21]. All polarization scans were conducted by increasing the cell potential from the open circuit value (+0.037 mV vs SCE on the freshly plated copper) to −1.2 V at a scan rate of 5 mV s^{-1}. At least two polarization scans were conducted for each set of conditions on separate days using freshly prepared suspensions and electrodes. Limiting current density values were obtained from repeated scans which were within ±5 mA cm^{-2}.

3. Results and discussion

Polarization scans were used to study the effect of particle loading on the current–potential relationship over the entire codeposition range, from the kinetically-controlled to mass-transfer limitation. At the cathode, ohmic losses cause the measured potential drop to appear more negative than it actually is. Therefore, the measured overpotential was corrected by subtracting the *IR* drop from the cathodic overpotential [27]. The solution resistance, R (Ω), can be calculated for a concentric cylinder configuration according to [14]

$$R = \frac{1}{2\pi\kappa h} \times ln\left(\frac{r_o}{r_i}\right) \tag{5}$$

where r_o is the inner radius of the outer cylinder (the location of the reference electrode), r_i is the outer radius of the inner cylinder, and h is the height of the solution. The conductivity, κ (S cm^{-1}), of the plating bath is affected by the particle loading in solution. Conductivity was measured as a function of particle loading and found to decrease with increasing particle loading, as shown in Figure 1 with the corresponding increase in

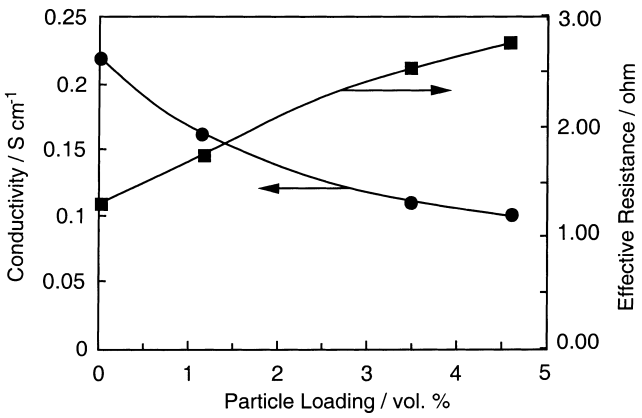

Fig. 1. Effect of particle loading on the conductivity and effective resistance of the deposition bath slurry.

resistance, calculated using Equation 5 for the case where the cathode was the inner rotating electrode. The large decrease in solution conductivity is due to the adsorption of ions on the alumina particles. Adsorption [28] and zeta potential [28, 29] measurements of alumina powder in acid copper sulfate have shown that both Cu^{2+} and SO_4^{2-} are adsorbed onto the alumina particle surface.

The effects of particle loading on the overall cathodic polarization scans are shown in Figures 2 and 3 at an electrode rotational rate of 1000 and 1500 rpm, respectively. Generally, a decrease in current density for a given potential in the kinetically-controlled and mixed-control regions is observed in the presence of particles. The addition of solid particles decreases the effective concentration of reactant, increases the effective viscosity, and decreases the cross-sectional area available for mass flux. However, as shown in Figures 2 and 3 the effects observed are not systematic with particle loading or rotational rate. As illustrated in Figures 2 and 3, the current density (or rate of deposition) is decreased with the addition of particle in the kinetically-limited region

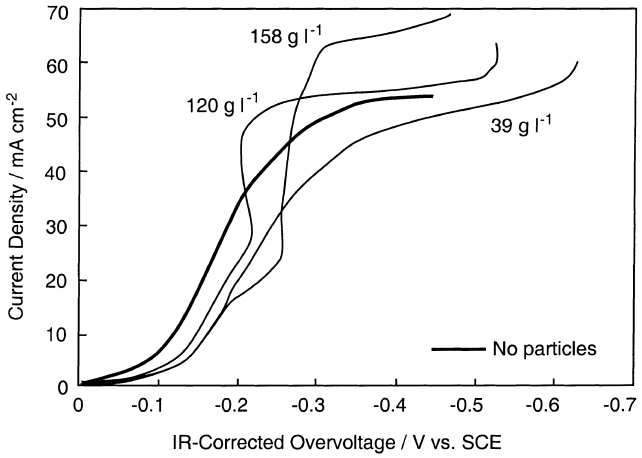

Fig. 2. Effect of particle loading on polarization scans at an electrode rotational rate of 1000 rpm.

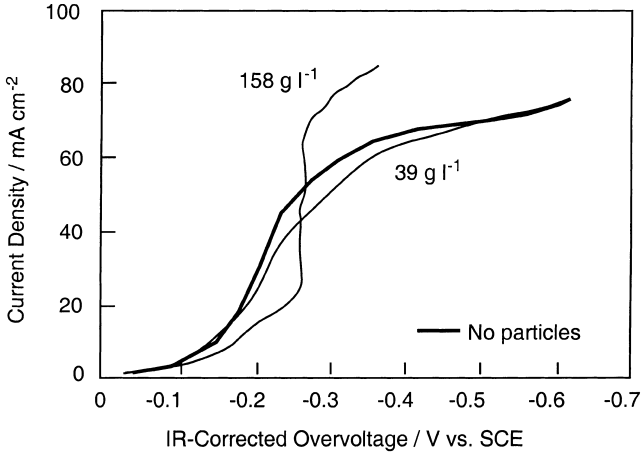

Fig. 3. Effect of particle loading on polarization scans at an electrode rotational rate of 1500 rpm.

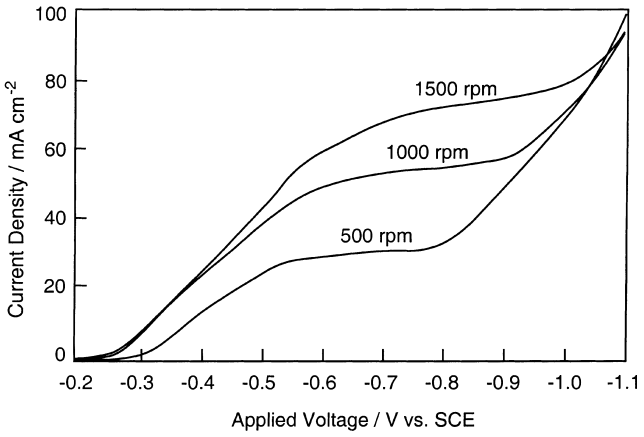

Fig. 4. Effect of electrode rotational rate on limiting current density.

($<\sim -0.2$ V). However, under mass transfer control with the addition of particles, even when being incorporated into the depositing film, the mass transfer is not decreased, but remains the same as without particles with low particle loading and even some enhancement at higher solids contents (158 g l^{-1}).

According to the ETW correlation of Equation 1 , the rate of mass transfer increases with the electrode rotational rate to the 0.7 power. The polarization scans obtained with 0.1 M $CuSO_4$ + 1.2 M H_2SO_4 as a function of rotational rate are shown in Figure 4. The experimental limiting current densities from Figure 4 are listed in Table 1. At each electrode rotational rate, the experimental and calculated values from Equation 1 matched exactly using $D = 0.52 \times 10^{-5}$ cm^2 s^{-1} and $\nu = 0.01$ cm^2 s^{-1} [30].

The effect of that 50 nm diameter alumina particle loading on the limiting current density was investigated with particle loadings of 3.9, 19.5, 39, 120 and 158 g l^{-1} at electrode rotational rates of 500, 1000 and 1500 rpm, which conditions were used for the codeposition experiments [21, 22]. The results of the effect particle loading on the limiting current density are summarized in Table 2.

It was found that particle loadings up to 120 g l^{-1} had no effect on the limiting current density. However, for a particle loading of 158 g l^{-1} the mass transfer is enhanced by 14, 32 and 19% at 500, 1000 and 1500 rpm, respectively. The decrease in the enhancement factor at rotational rates of 1500 rpm may be due to increased particle–particle interactions at the higher rotational rate creating interference which hinders the enhance-

Table 1. Experimental limiting current density (i_L) for 0.1 M $CuSO_4$ + 1.2 M H_2SO_4

Rotational rate /rpm	Experimental i_L /mA cm^{-2}
500	31
1000	50
1500	67

Table 2. Effect of particle loading on the ratio of limiting current density with and without particles (i_L^*/i_L)

Rotational rate /rpm	Particle loading /g l^{-1}	i_L^*/i_L		
		Experimental	Equation 3†	Equation 4‡
500	3.9	1.00	2.9	*
	19.5	1.00	3.0	*
	39	1.00	3.1	1.1
	120	0.95	3.4	1.5
	158	1.14	3.5	1.7
1000	3.9	1.00	2.8	*
	19.5	1.00	2.9	1.0
	39	1.00	3.0	1.1
	120	1.00	3.3	1.5
	158	1.32	3.4	1.7
1500	3.9	1.00	2.8	*
	19.5	1.00	2.9	1.0
	39	1.00	3.0	1.1
	120	1.00	3.3	1.6
	158	1.19	3.4	1.7

* A ratio <1 was predicted

† The following functions of ϕ were used: $\alpha = 0.016 + 0.16\,\phi$ and $\beta = 0.38 + 0.31\,\phi$ [20]

‡ The following functions of ϕ was used: $\alpha = 0.0093 + 0.195\,\phi$ [20]

ment of the mass transfer relative to the enhancement obtained at 1000 rpm.

The enhancements of limiting current density predicted by Equations 3 and 4 were calculated. Linear relationships for α and β as a function of particle volume fraction were determined from the data given in [20] to extrapolate to the small values used in our experiments. The calculated values of the limiting current density enhancement are also reported in Table 2. All of the values calculated by Equation 3 show a large enhancement in mass transfer of 2.9–3.5 with particles in solution. Considering that agglomeration may take place with these small particles, the particle size necessary to give the observed values of limiting current density was determined to be of the order of 100 times larger ($\sim$5 μm). The values calculated from Equation 4 show an enhancement with loadings of 39 g l^{-1} or greater, which although lower than the values determined from Equation 3, still overestimate the observed enhancement. The particle size necessary to give observed mass transfer enhancement is only on the order of 10 times the actual particle size of 50 nm, which may be an effective size considering agglomeration. The dry powder did have 0.5 μm diameter agglomerates, but the size of the incorporated particles was confirmed by scanning electron microscopy to remain 50 nm in diameter [22, 23].

A critical value of the volume fraction and also the rotational rate above which particles affect the mass transfer has been observed for studies of the effect of suspended nonconducting particles on the mass transfer at a rotating disk electrode [30]. A model was developed to explain this result [31]. The model shows a linear relationship with particle volume fraction above a critical value; this critical value of volume fraction is stated to be due to a gravitational effect in which the minimal approach distance between particles and the rotating electrode become smaller than the diffusion boundary layer thickness. The threshold rotational rate was shown to be inversely proportional to particle size, which would indicate that for very small particles such as used in this study the critical value for the electrode rotational rate would be very high and beyond practical application.

5. Conclusions

The effect of particle loading on the polarization behavior during coelectrodeposition of nanometric diameter alumina with copper with a rotating cylinder electrode from the kinetically-controlled to mass-transfer limitation conditions was studied with an optimal electrolytic bath composition of 0.1 M $CuSO_4$ + 1.2 M H_2SO_4, which was used in coelectrodeposition experiments [22]. In the kinetically-controlled region, the particles in suspension led to a decrease in the current for a given potential value compared without particles in suspension for all particle loadings. For mass transfer limiting conditions, alumina particle loadings at or below 120 g l^{-1} had no effect. However, a particle loading of 158 g l^{-1} was found to increase the limiting conditions by as much as 32%.

Acknowledgements

This research was supported in part by the American Electroplaters and Surface Finishes Society (AESF), Graduate Women in Science-Sigma Delta Epsilon, and a Patricia Harris Fellowship. David Wang is thanked for his limiting current density measurements.

References

1. M. Viswanathan, *Metal Finish.* **71** (1973) 38.
2. J.R. Roos, J.P. Celis and J.A. Hensen, *Trans. Inst. Metal Finish.* **55** (1977) 113.
3. D.W. Snaith and P.D. Groves, *Trans. Inst. Metal Finish.* **56** (1978) 9.
4. J.P. Celis, H. Kelchtermans and J.R. Roos, *Trans. Inst. Metal Finish.* **56** (1978) 41.
5. C. White and J. Foster, *Trans. Inst. Metal Finish.* **59** (1981) 9.
6. C. Buelens, J.P. Celis and J.R. Roos, *J. Appl. Electrochem.* **13** (1983) 541.
7. V.P. Greco, *Plat. Surf. Finish.* **76** (1989) 68.
8. G.A. Malone, *Plat. Surf. Finish.* **78** (1991) 58.
9. S.W. Watson and R.P. Walters, *J. Electrochem. Soc.* **138** (1991) 3633.
10. H. Hayashi, S. Izumi and I. Tari, *J. Electrochem. Soc.* **140** (1993) 362.
11. P.R. Webb and N.L. Robertson, *J. Electrochem. Soc.* **121** (1994) 669.
12. R. Bazzard and P.J. Boden, *Trans. Inst. Metal Finish.* **50** (1972) 63.

13. B.J. Hwang and C.S. Hwang, *J. Electrochem. Soc.* **140** (1993) 979.
14. M. Eisenberg, C.W. Tobias and C.R. Wilke, *J. Electrochem. Soc.* **101** (1954) 306.
15. J.S. Newman, 'Electrochemical systems' (Prentice Hall, New Jersey, 1973).
16. D.R. Gabe and D.J. Robinson, *Electrochim. Acta* **17** (1972) 1129.
17. D.R. Gabe and D.J. Robinson, *Trans. Inst. Metal Finish.* **49** (1971) 17.
18. D.J. Robinson and D.R. Gabe, *Trans. Inst. Metal Finish.* **48** (1970) 35.
19. R. Kappesser, I. Cornet and R. Greif, *J. Electrochem. Soc.* **118** (1971) 1957.
20. D.W. Gibbons, R.H. Muller and C.W. Tobias, *J. Electrochem. Soc.* **138** (1991) 3255.
21. J.L. Stojak, PhD thesis, University of California, San Diego (1997).
22. J.L. Stojak and J.B. Talbot, *J. Electrochem. Soc.* **146** (1999) 4504.
23. A.J. Arvia and J.S.W. Carrozza, *Electrochim. Acta* **7** (1962) 65.
24. J.C. Bazan and A.J. Arvia, *Electrochim. Acta* **9** (1964) 17.
25. L.J.J. Janssen and J.G. Wijers, *J. Appl. Electrochem.* **19** (1989) 823.
26. J.R. Selman and C.W. Tobias, *Adv. Chem. Eng.* **10** (1978) 211.
27. S. Barnartt, *J. Electrochem. Soc.* **108** (1961) 102.
28. H. Hayashi, S. Izumi and I. Tari, *J. Electrochem. Soc.* **140** (1993) 362.
29. C.C. Lee and C.C. Wan, *J. Electrochem. Soc.* **138** (1988) 1930.
30. R. Caban and T.W. Chapman, *J. Electrochem. Soc.* **124** (1977) 1371.
31. P.J. Sonnevald, W. Visscher and E. Barendrecht, *J. Appl. Electrochem.* **20** (1990) 563.